SAND2020-6267PE

Molecular Simulation of Nanoparticle-Nanopore Interactions: Adsorption, Aggregation and Fracture

Louise Criscenti
Geochemistry Department
Sandia National Laboratories
Albuquerque, NM 87185

U.S. DEPARTMENT OF ENERGY | Office of Science

Built on LDRD Laboratory Directed Research

SAND2019-14116 PE

Sandia National Laboratories is a multimission laboratory managed and operated by National Technology & Engineering Solutions of Sandia, LLC, a wholly owned subsidiary of Honeywell International Inc., for the U.S. Department of Energy's National Nuclear Security Administration under contract DE-NA0003525.

Sandia National Laboratories is a multimission laboratory managed and operated by National Technology and Engineering Solutions of Sandia LLC, a wholly owned subsidiary of Honeywell International Inc. for the U.S. Department of Energy's National Nuclear Security Administration under contract DE-NA0003525.

Sandia's History

Exceptional service in the national interest

- July 1945: Los Alamos creates Z Division
- Nonnuclear component engineering
- November 1, 1949: Sandia Laboratory established

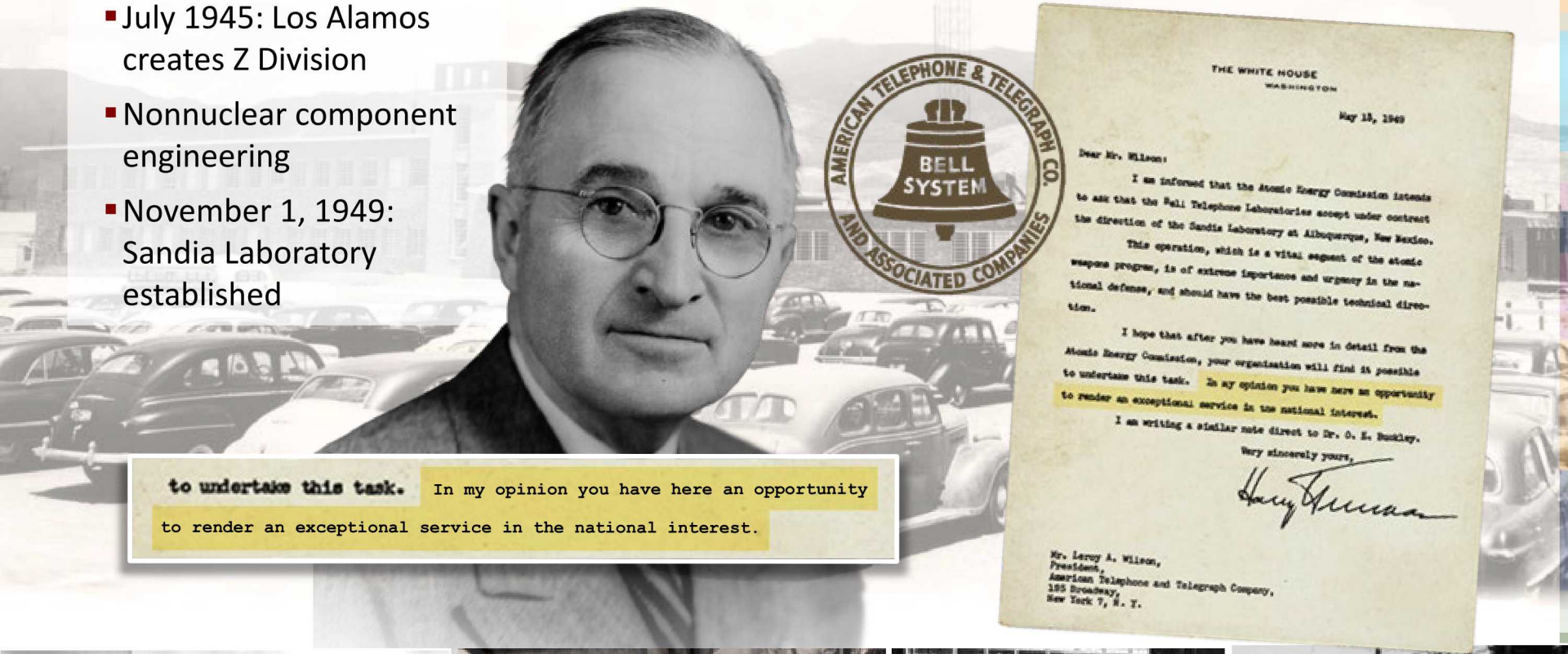

to undertake this task. In my opinion you have here an opportunity to render an exceptional service in the national interest.

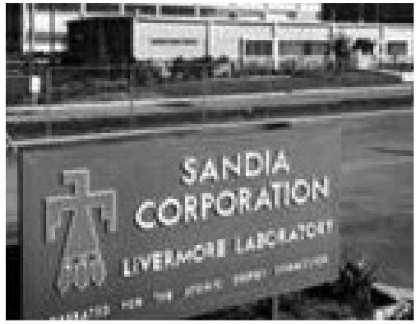

Sandia National Laboratories Highlights

Sandia Mission Focus

- Nuclear Deterrence
- National Security Programs
- Integrated Security Systems (Energy, Climate)
- Defense Nuclear Nonproliferation
- Advanced Science & Technology

Government-owned, contractor-operated
Federally funded research and development center






Six sites – NM, TX, CA, NV, HI

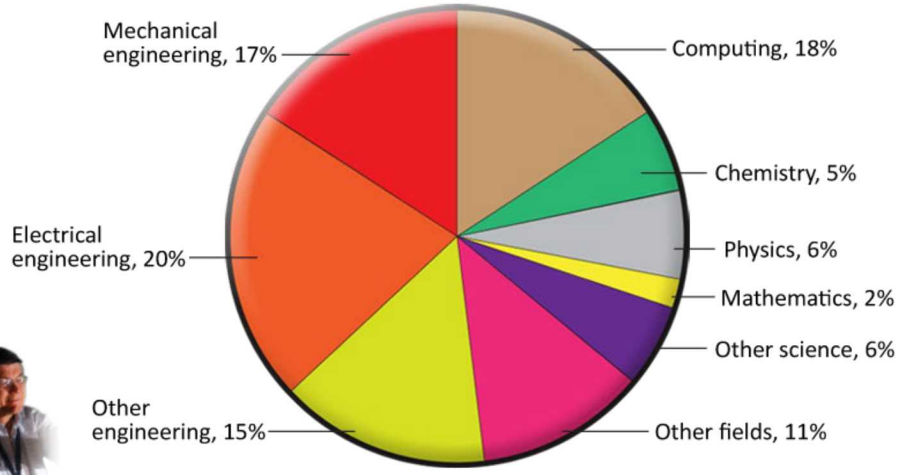

~11,000 employees, ~5000 technical staff

Louise Criscenti - Biography

1. Needham High School, Needham, MA
2. B.S. Brown University, Providence RI
3. M.S. University of Washington, Seattle, WA
    - Stillwater Complex (Igneous Petrology, McCallum)
4. Research Scientist, PNNL, Richland, WA
    - Geochemical modeling, Reactive-Transport modeling for contaminant migration problems
    - Stint at EPA, Athens, GA
5. Ph.D. Johns Hopkins University, Baltimore, MD
6. Postdoc PennState, University Park, PA
    - Brantley & Kubicki
    - Gaussian calculations
    - Kinetic reaction paths of silicate dissolution
7. Sandia National Laboratories
    - Postdoc (Cygan; Force field modeling)
    - Permanent Staff

Current Projects: Contract Research

Lead PI: Interfacial Geochemistry of Nano-scale Pores: Molecular Behavior in Subsurface Environments. (BES)

- REE adsorption to silica nanopores; water structure in silica nanopores, & gibbsite particle aggregation

Acting Lead PI: Development of a Tightly Coupled Multi-Physics Numerical Model for an Event-Based Understanding of Arctic Coastal Erosion (LDRD)

- "This project will deliver a field-validated predictive model of thermo-chemical-mechanical erosion for the permafrost Arctic coastline."

Strategic Petroleum Reserves (US DOE FE)

- Long-term (>30-years) project at SNL, maintaining petroleum reserves in salt caverns for the federal government
- PHREEQC calculations to investigate potential dissolution of caprock overlying one cavern.

DOE NE Nuclear Waste Forms

- Investigate nuclear waste glass degradation data and models for potential incorporation into repository risk assessment models.

Plasma Physics Grand Challenge LDRD

- Desorption of H_2O and Steel Corrosion under ultrahigh vacuum and high T (1000K)

Permafrost exposed by coastal erosion along the Beaufort Sea (credit: K. Dunton, Univ. of Texas)

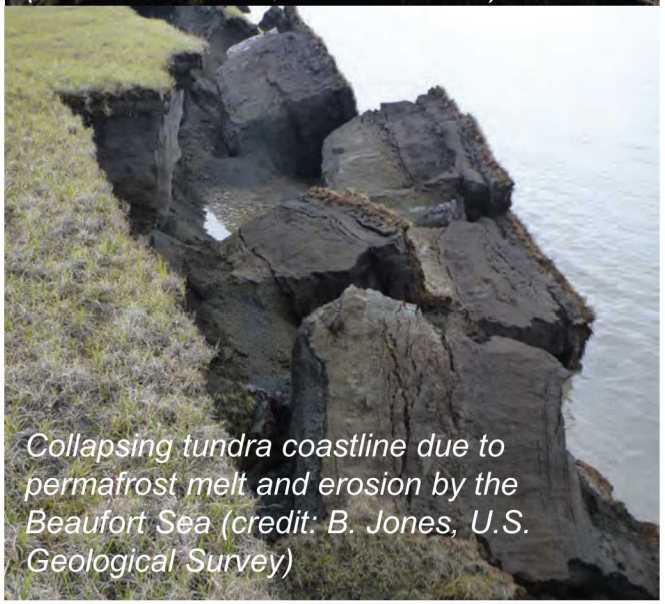

Collapsing tundra coastline due to permafrost melt and erosion by the Beaufort Sea (credit: B. Jones, U.S. Geological Survey)

Modeling Nanoaggregates: Kerogen

Van Krevelen diagram

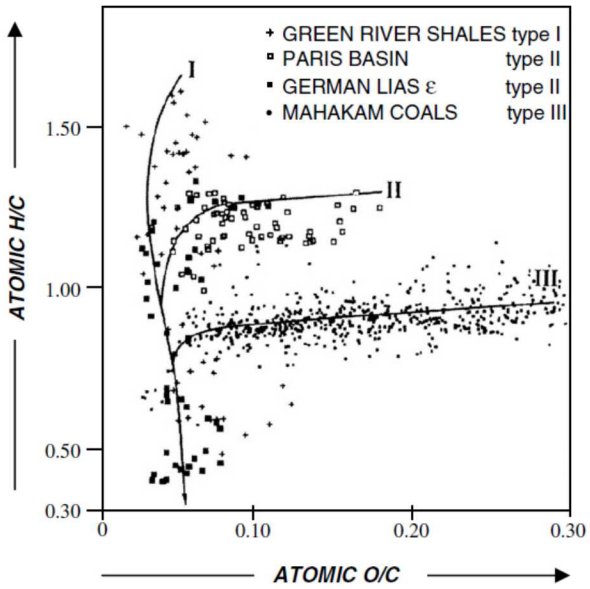

Vandenbroucke, Org. Geochem. 38, 719-833 (2007)

> Maturation
> Aromaticity
< Functional Groups

O
N
S
H
C

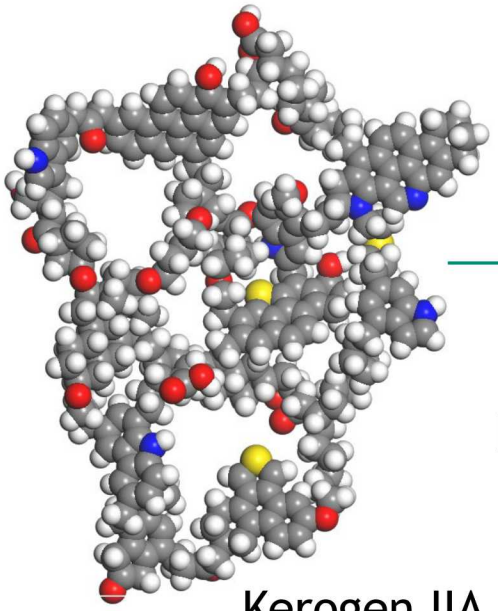

Kerogen IIA

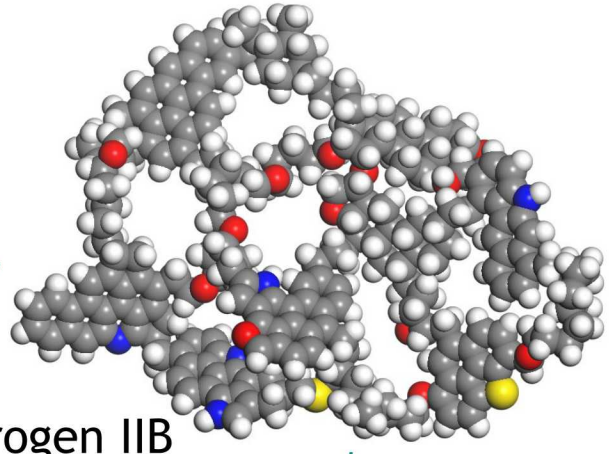

Kerogen IIB

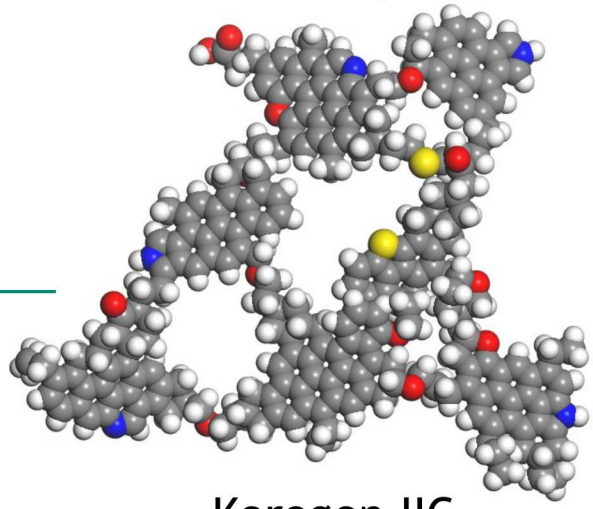

Kerogen IIC

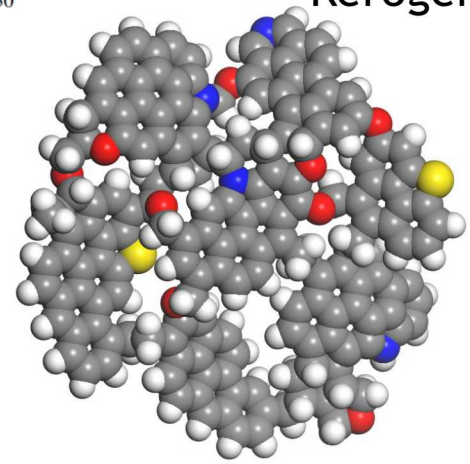

Kerogen IID

Ungerer et al., Energy & Fuel 29, 91-105

Formation of Condensed Kerogen

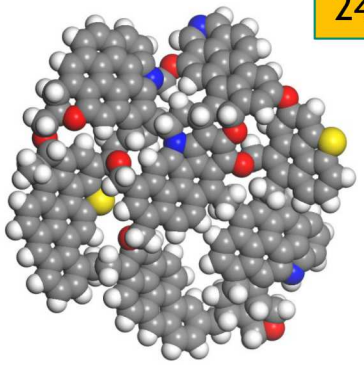

$C_{175}H_{102}O_9N_4S_2$

Ungerer et al. 2015
Energy Fuels 29, 91-105

24 Kerogens in 10x10x10nm^3 box, 1000K

NVT

9 snapshots

NPT, 100atm 900K to 300K

300K and 100atm

NPT, 1atm, *300K*

9 samples at 300K and 1atm

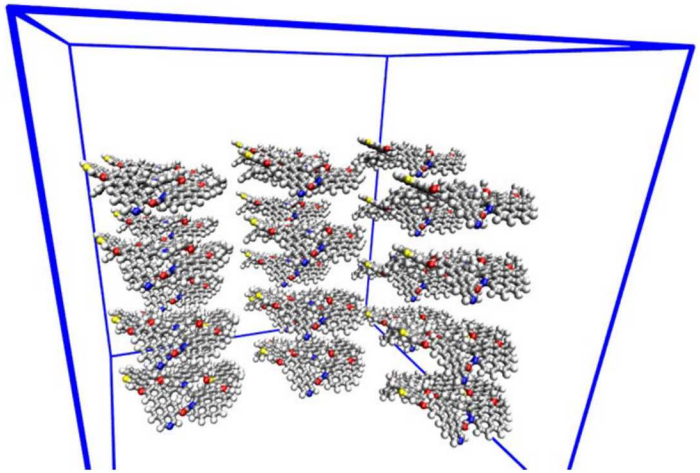

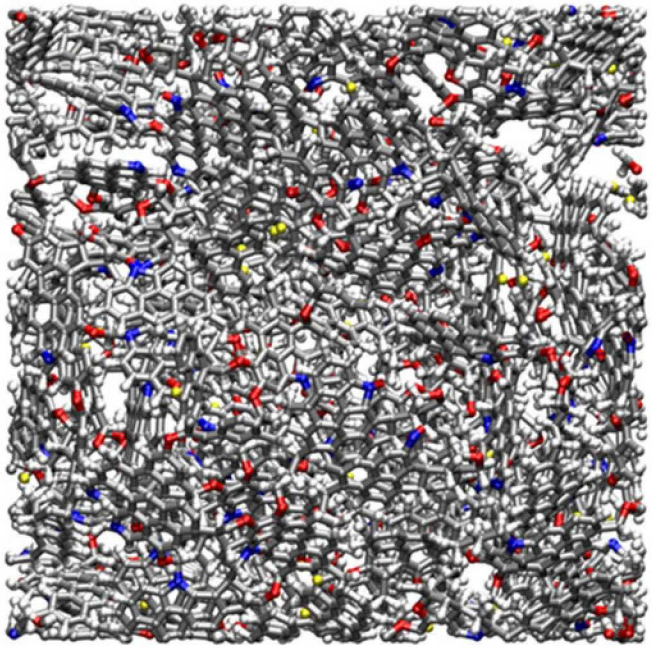

Characterization

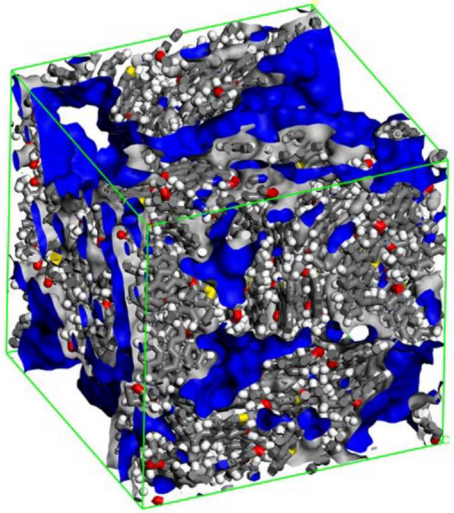

Density

Sample 1: 1.172g/cm^3
Sample 2: 1.287g/cm^3
Average: 1.22±0.04 g/cm^3
Experiment: 1.28±0.3g/cm^3

Stankiewicz A, *et al.* (2015) Kerogen density revisited – lessons from the Duvernay Shale. *In: Paper URTeC 2157904 at the Unconventional Resources Technology Conference, San Antonio, Texas, July 2015*

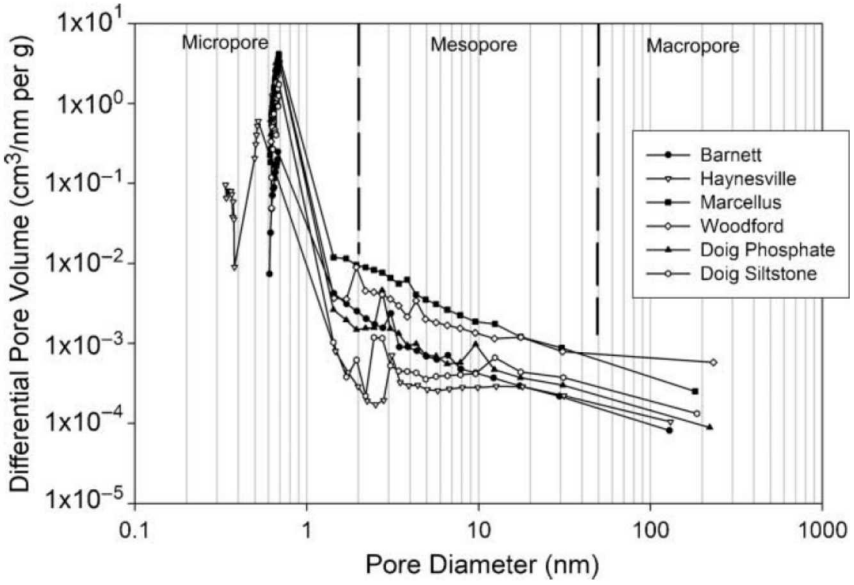

Chalmers et al. (2012) AAPG 96, 1099-1119

Pore size distribution

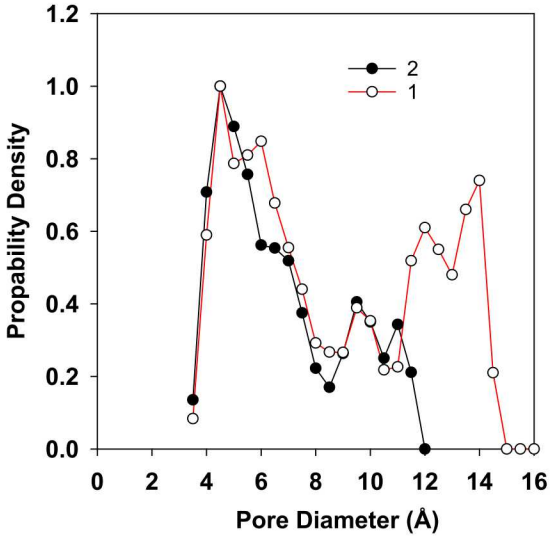

Method: Bhattacharya S & Gubbins KE (2006) *Langmuir* 22:7726-7731

Methane extraction from kerogen

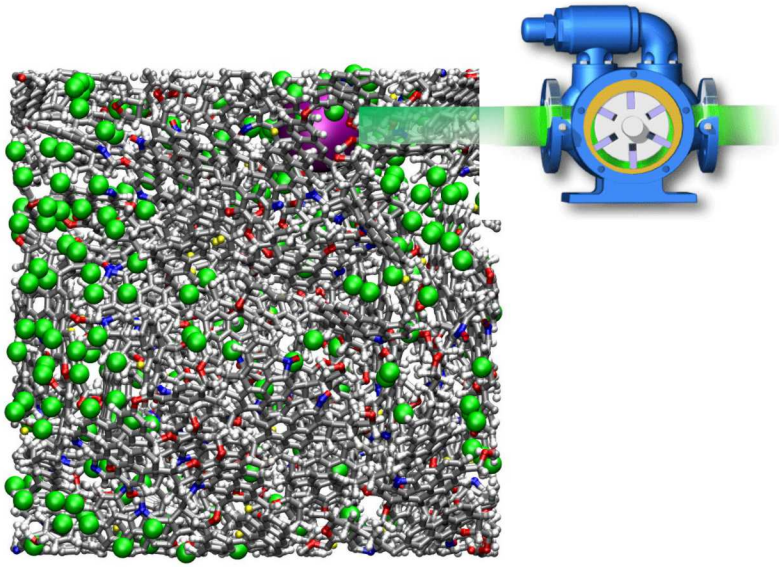

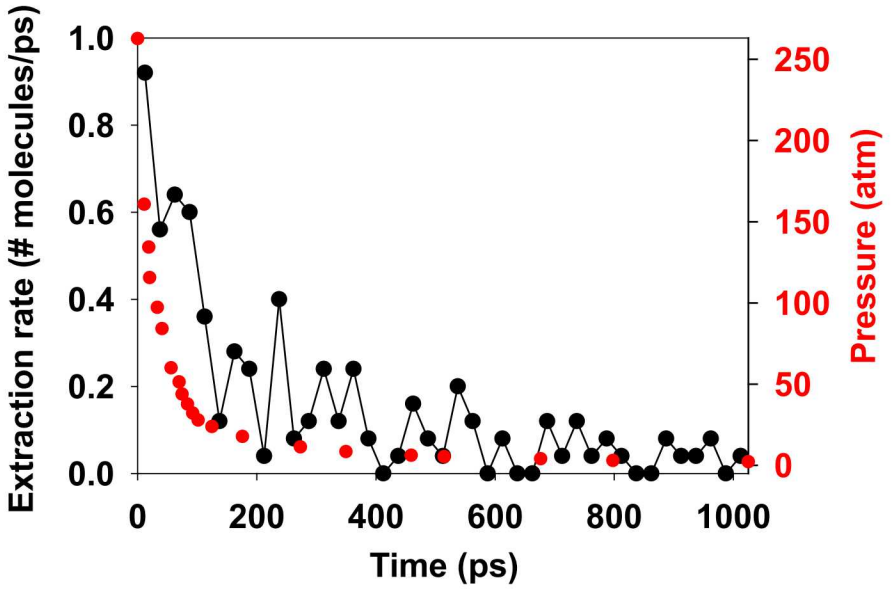

- Two stages of gas release
- Pore network connectivity can significantly affect the ultimate recovery

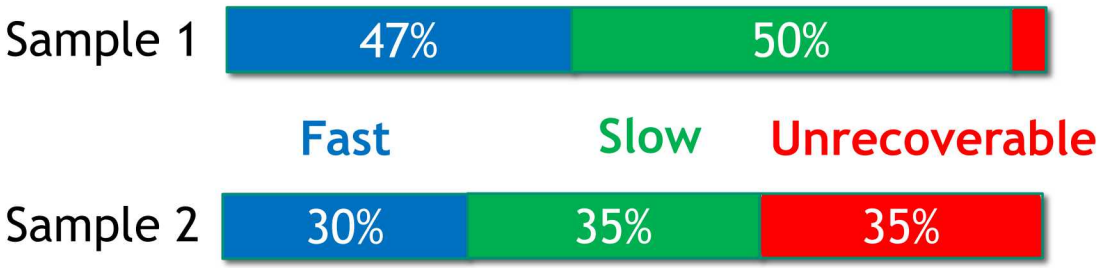

Ho et al. (2016) Nature Scientific Reports, DOI: 10.1038/srep28053

Towards Ion Adsorption and Diffusion in Clay-Rich Rocks

- The objective is to use molecular simulation to investigate aqueous ion diffusion and adsorption to mineral surfaces in complex systems that are more representative of compact soils and rocks.
- Gibbsite is used as a model mineral because it has properties similar to a clay mineral but does not include the additional complexity of an interlayer.
- Molecular simulations are performed for:
  - Water and ion adsorption to the basal (001) and edge (100) gibbsite surfaces
  - Water and ion adsorption to a gibbsite nanoparticle
  - Water adsorption to gibbsite nanoparticle aggregates that are created through de-watering and compaction

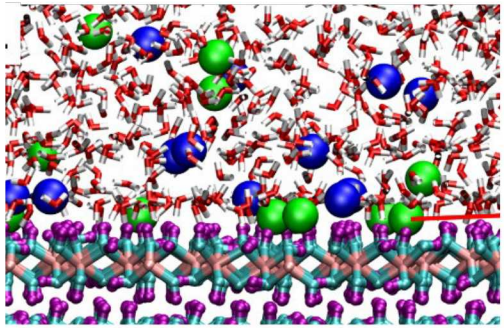

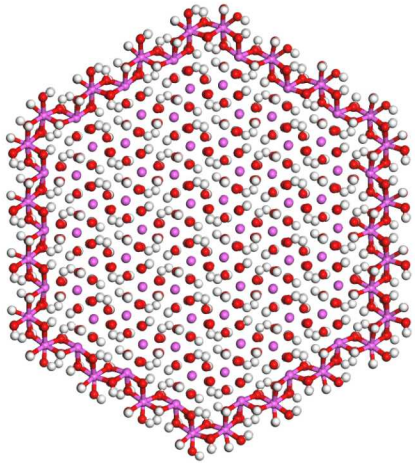

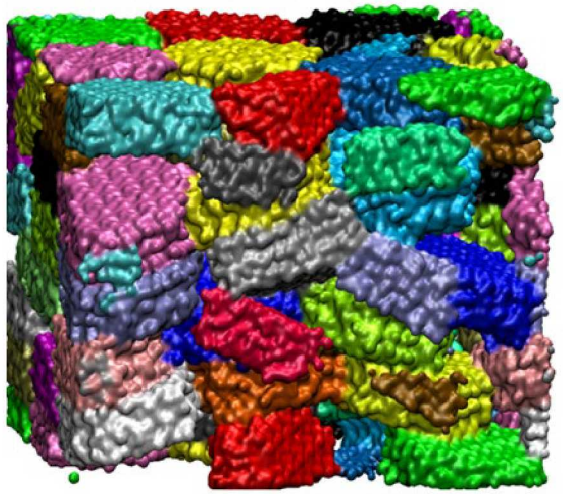

Gibbsite nanoparticle construction

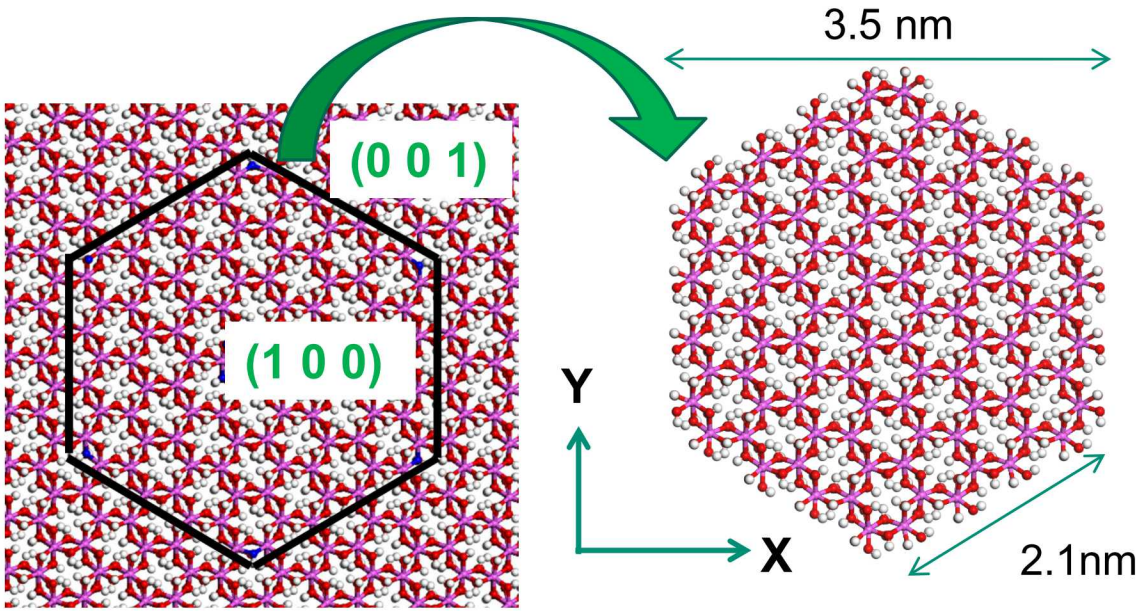

Lateral dimension 2.1 – 3.5 nm
Particle thickness 3 layers (1.3 nm)

Exploit the hexagonal symmetry of bulk gibbsite

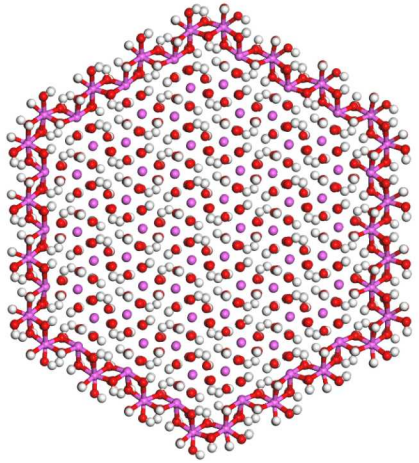

Molecular dynamics

- LAMMPS code with ClayFF parameters.
- New Al-O-H angle bending term for stability of edge sites.
- Extra Al-O-Al term added for nanoparticle stability.

Gibbsite aggregation

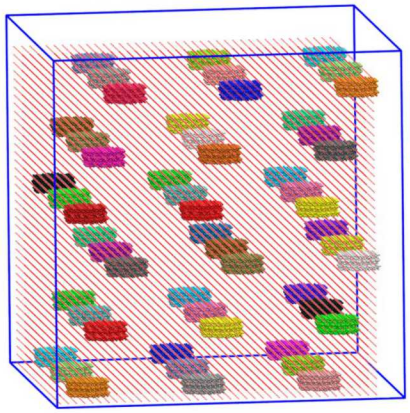

54 NPs, 55k H_2O
30 x 30 x 30 nm^3

NVT
0.3 ns
300 K

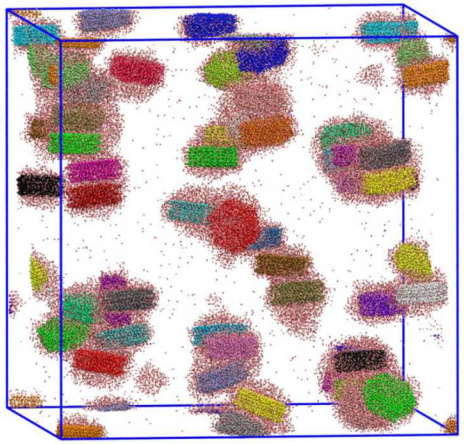

NPT
0.3 ns
300 K
100 MPa

Hydrated aggregate
15 x 15 x 15 nm^3

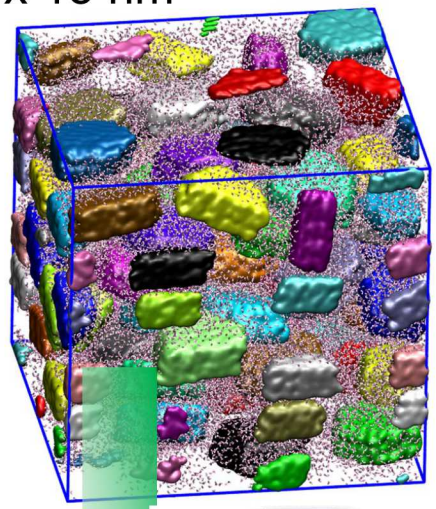

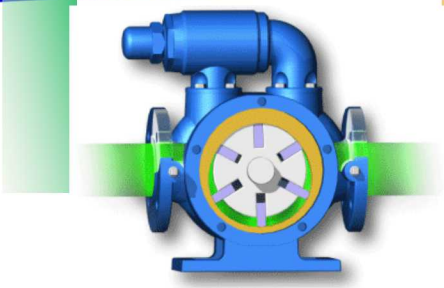

'Virtual' pump removes waters from a pre-defined region.

Effect of dewatering rate:

- Delete all water: "Fast"
- Delete 100 H2O/100 steps: "Intermediate"
- Delete 10 H2O/100 steps: "Slow"

Effect of water content:

- 1 water layer around each particle: 1W (22.5 wt%)
- 2 water layers around each particle: 2W (37.2 wt%)
- Additional withdraw water from 2W: 2W_dewatering (6 wt%)
- Dry: 2W_dry

Ho, T.A., Greathouse, J.A., Wang, Y. and Criscenti, L.J. (2017) Atomistic structure of mineral nano-aggregates from simulated compaction and dewatering. Scientific Reports 7:15286

Stacking of nanoparticles

"Fast"

"Slow"

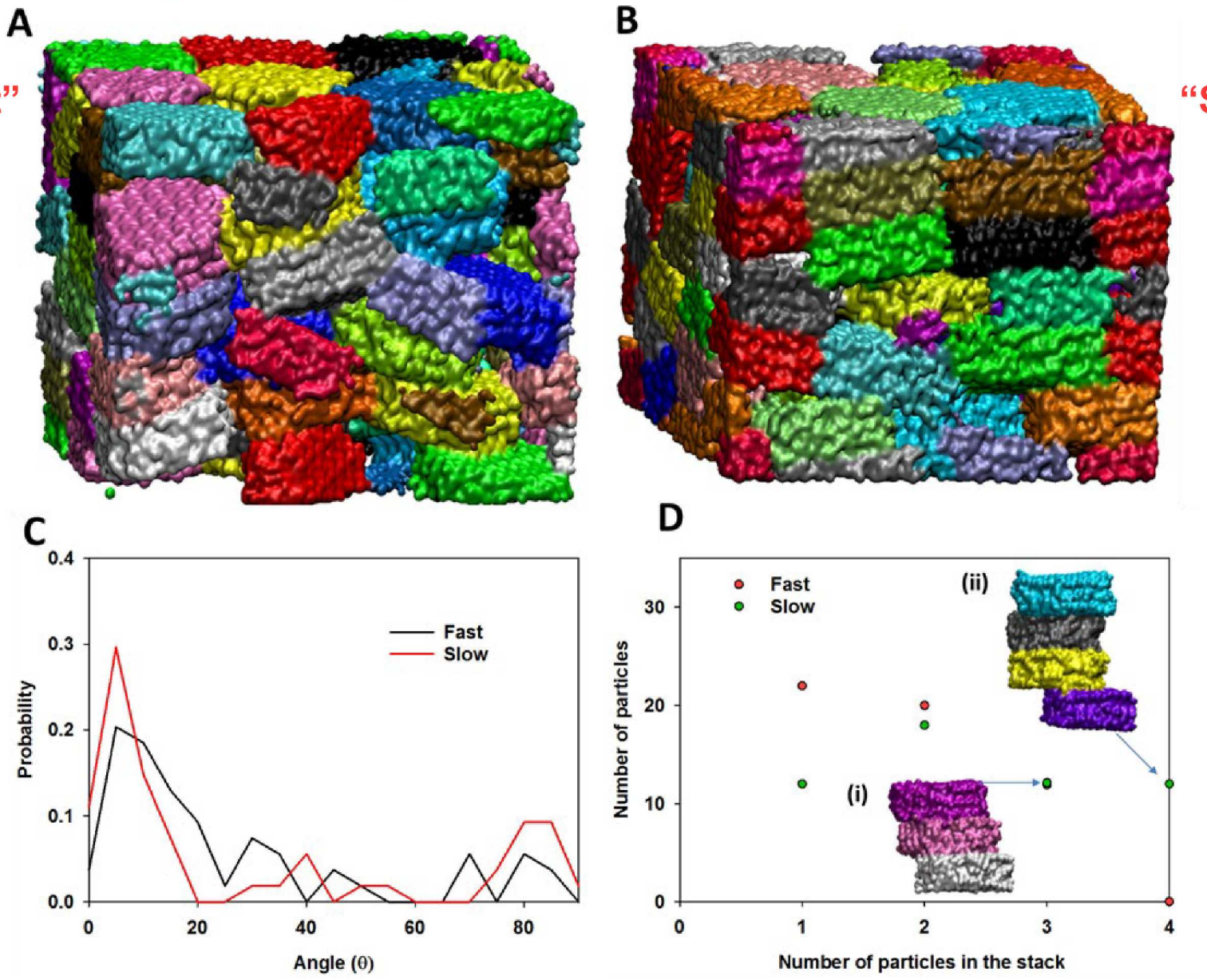

Ho et al. Scientific Reports 7:15286

Pore properties

Effect of dewatering on PSD

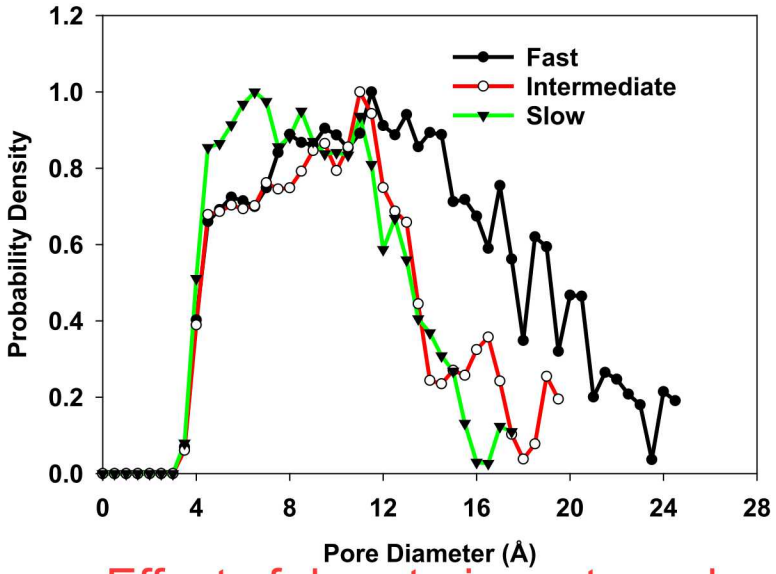

Effect of water content on PSD

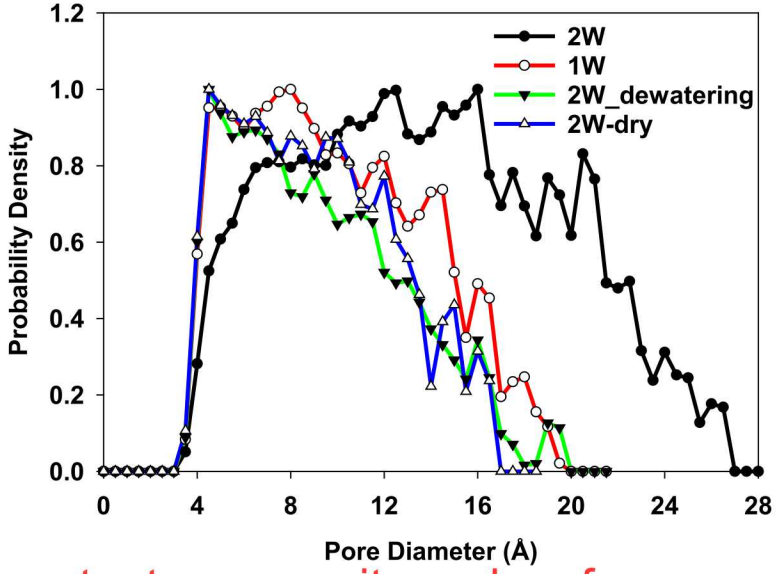

Effect of dewatering rate and water content on porosity and surface area

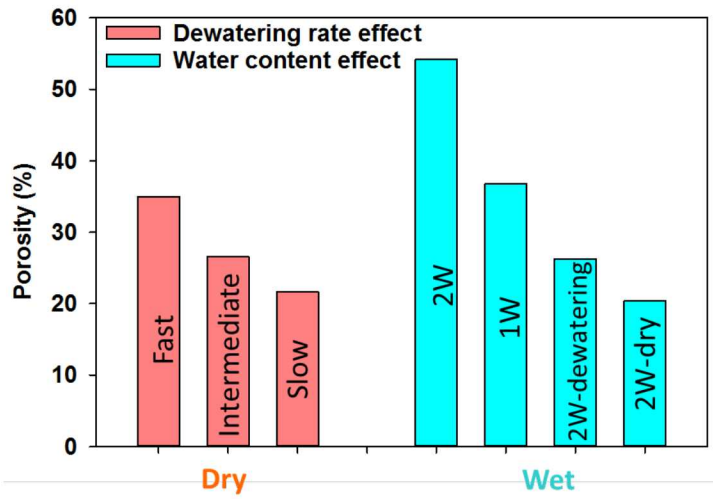

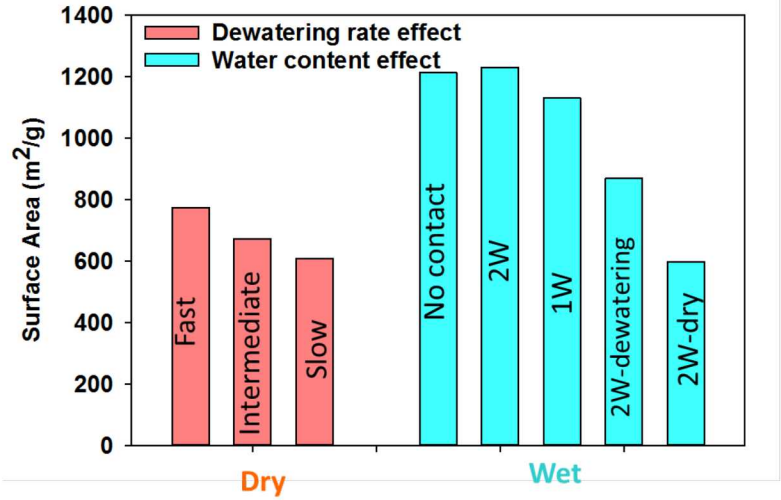

Ho et al.(2017) Scientific Reports 7:15286

Adsorption on Gibbsite basal (001) and edge (100) surfaces

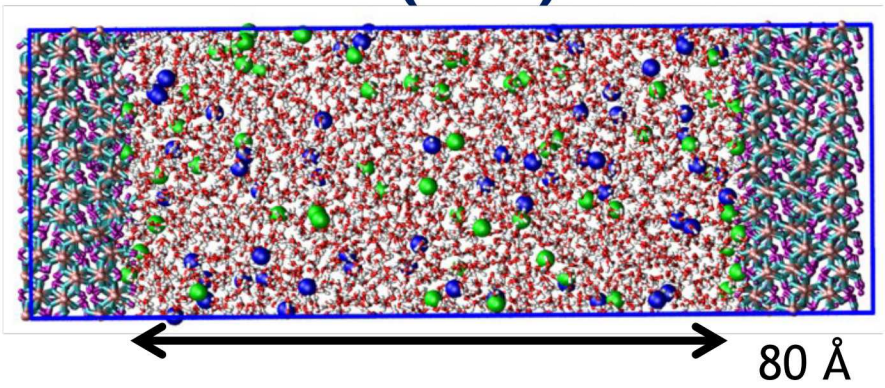

Molecular dynamics

- LAMMPS code with ClayFF force field.
- New Al-O-H angle bending term for stability of edge sites (Pouvreau et al., 2017)

Al
O
H
O_w
H_w
Na
Cl

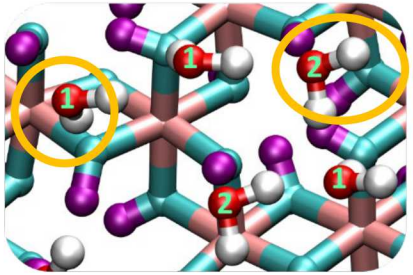

(001)

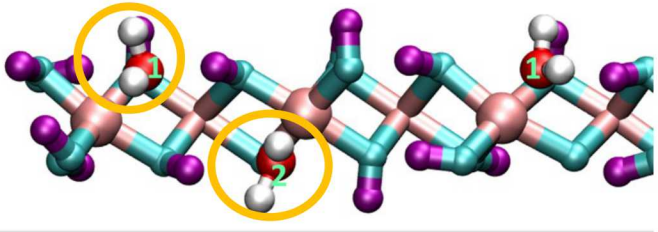

(100)

Water adsorption sites

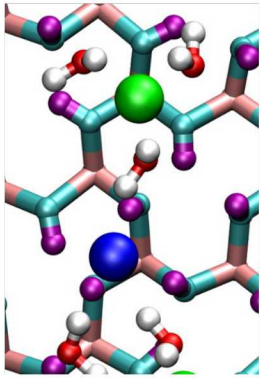

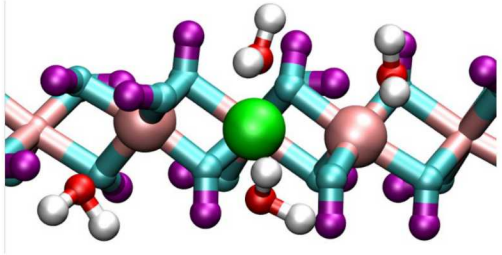

Ion adsorption sites

Ho, T.A., Greathouse, J.A., Lee, A.S. and Criscenti, L.J. (2018) Enhanced Ion Adsorption on Mineral Nanoparticles. Langmuir 34, 5926-5934.

Cation Adsorption to Gibbsite Surfaces

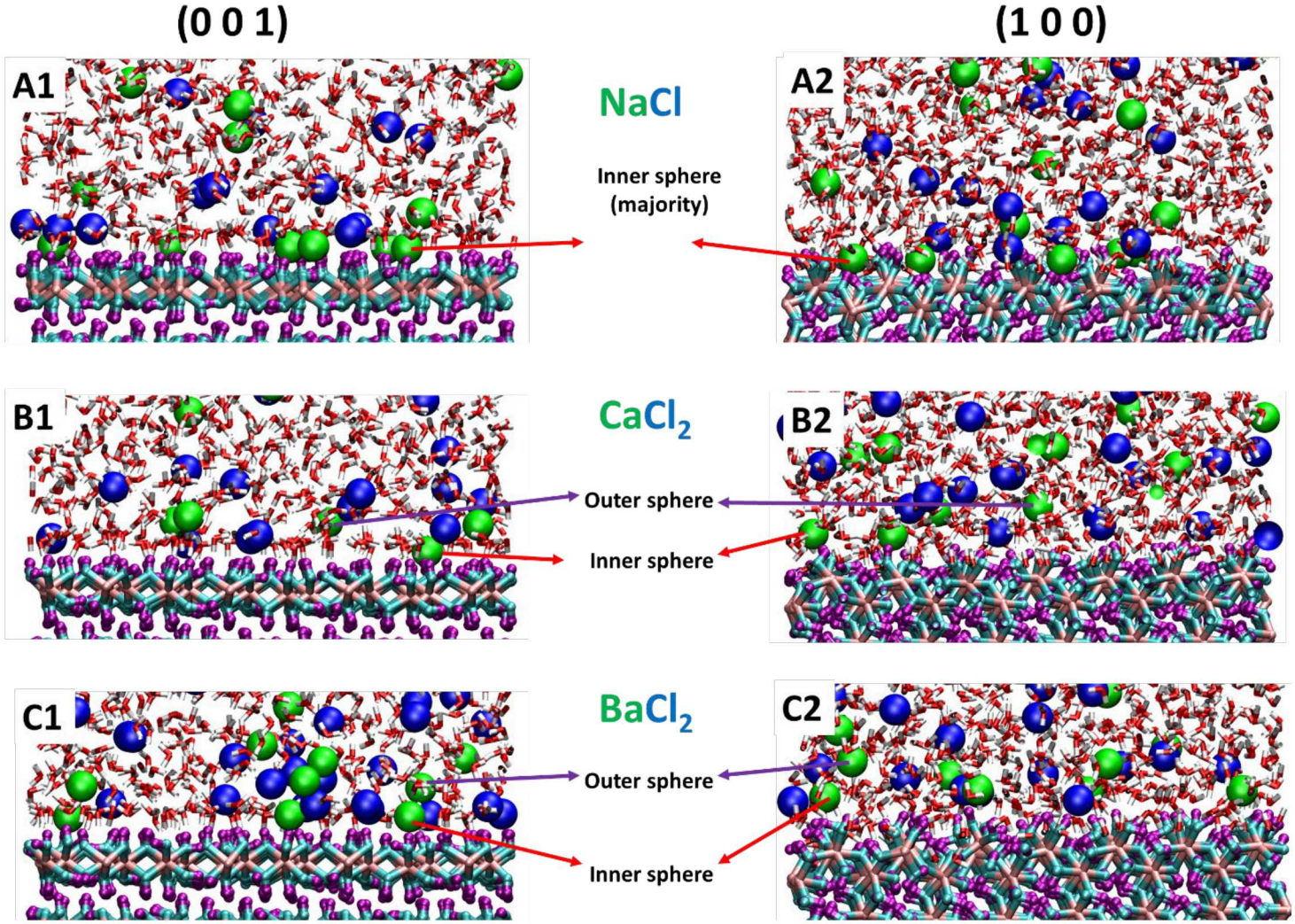

Ho, T.A. et al. (2018) Langmuir 34, 5926-5934.

Comparison of Adsorption on Gibbsite Nanoparticle vs. Surfaces

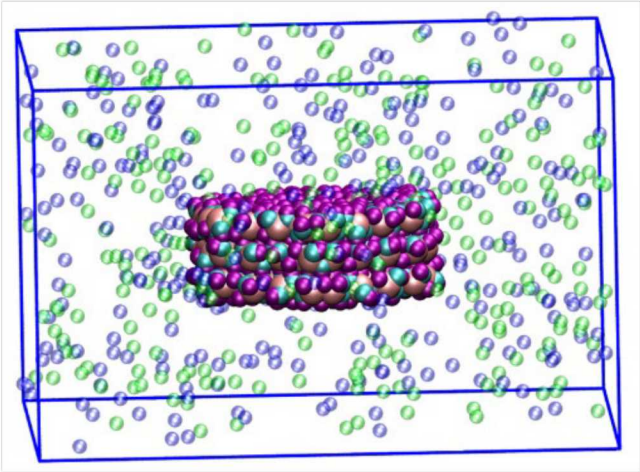

- Cl^- adsorption is not enhanced on NP
- Na^+, Ca^{2+}, and Ba^{2+} adsorption are enhanced on NP
- NPs exhibit higher concentrations of IS complexes

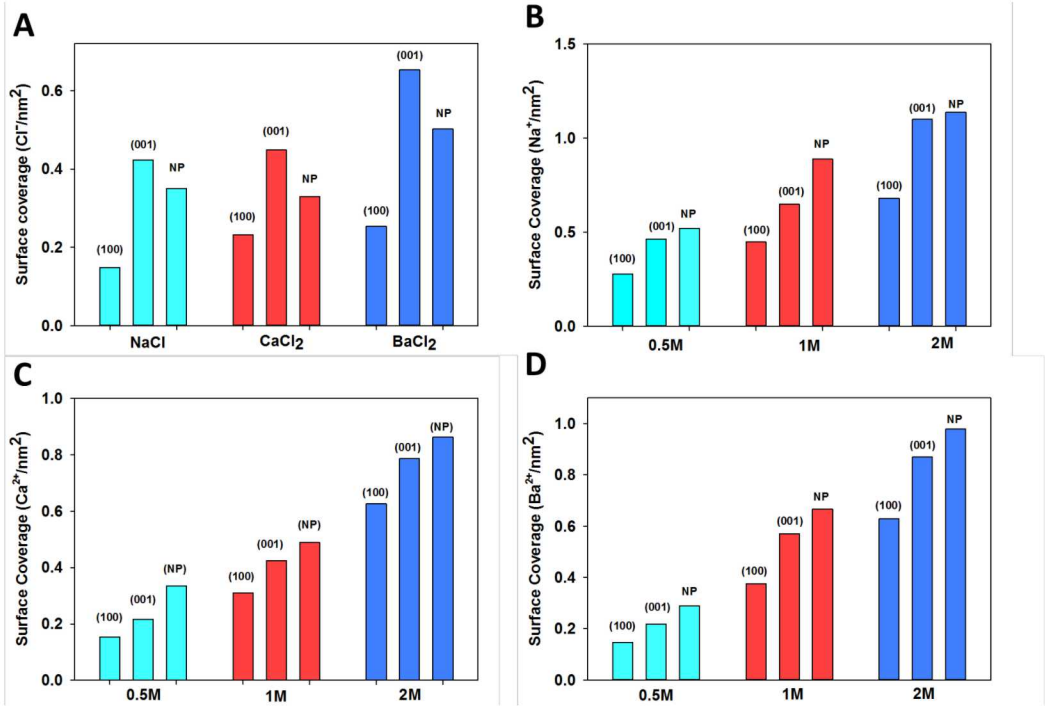

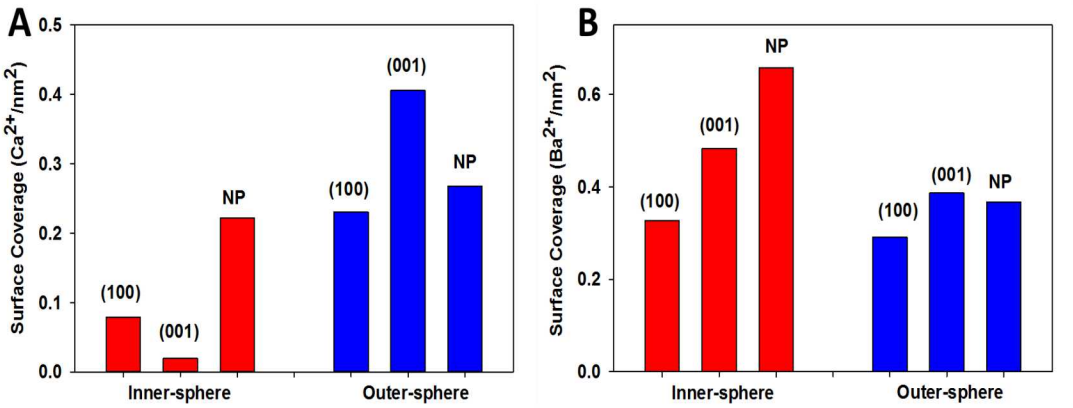

Ho, T.A. (2018) Langmuir 34, 5926-5934.

Cation Adsorption at Nanoparticle Corners

Snap-shots

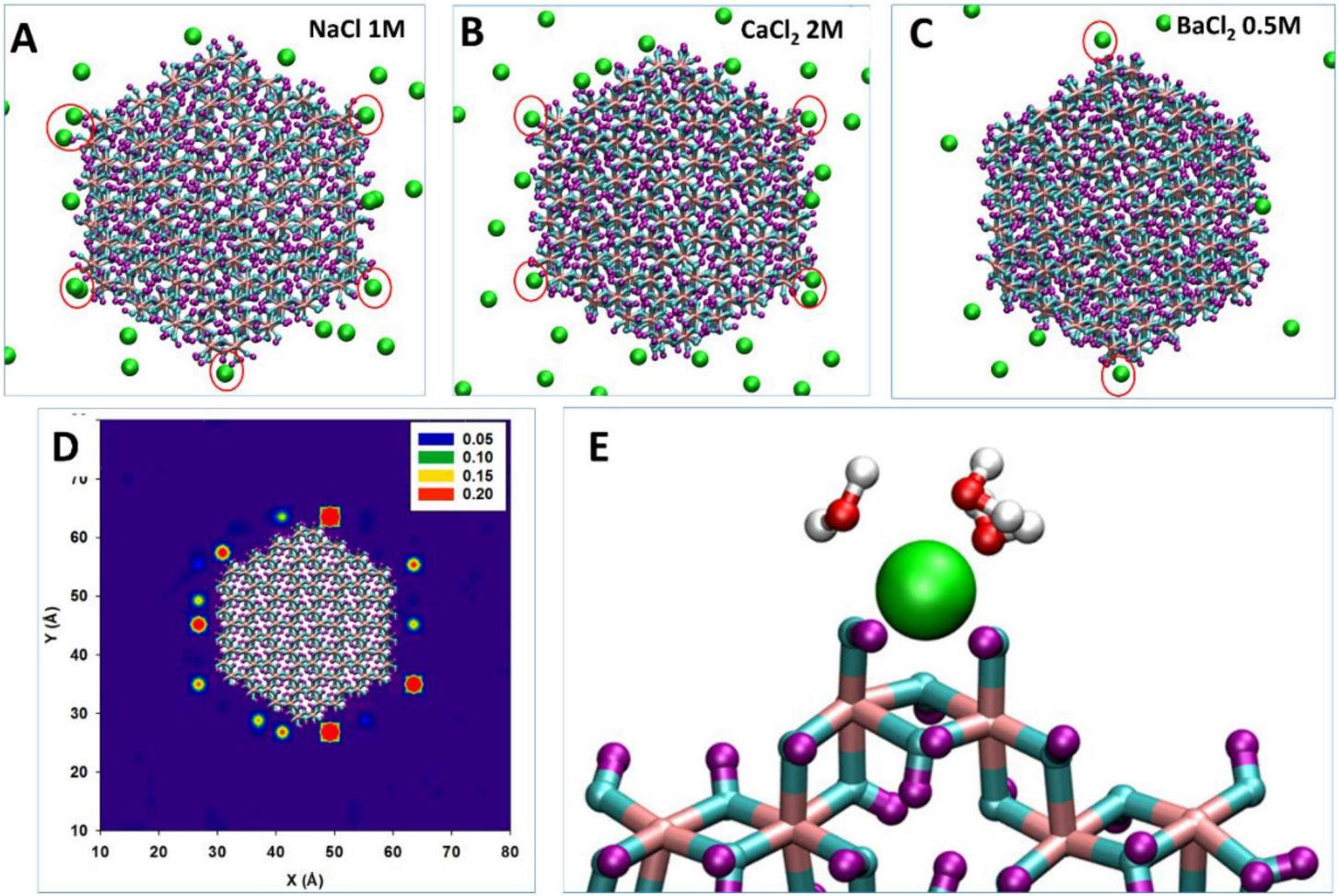

Planar density distribution
Na^+ over 10 ns

Ho, T.A. et al. (2018) Langmuir 34, 5926-5934.

Water structure: 1D atomic density profiles

2W water content (37 wt%)

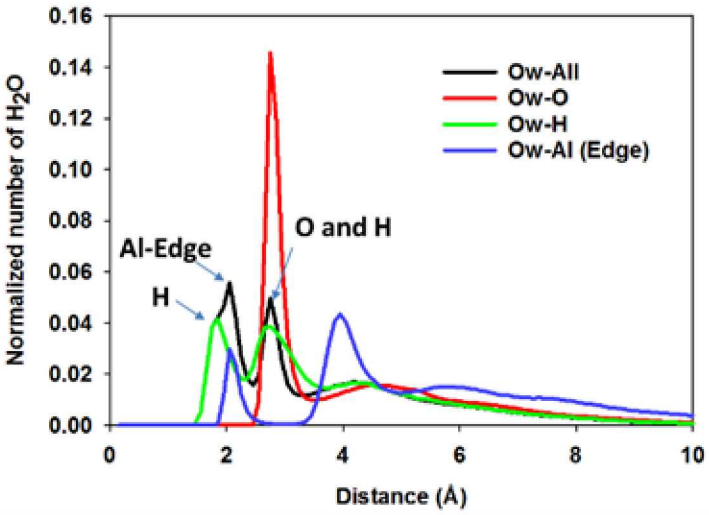

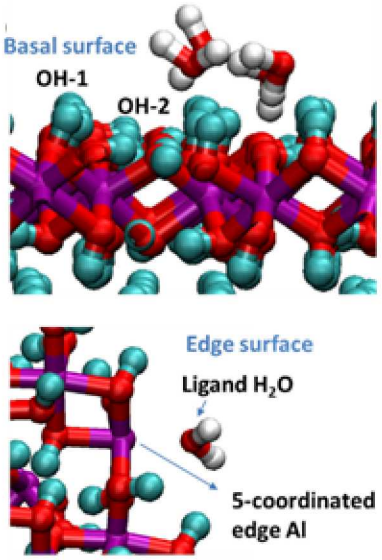

1W water content (22 wt%)

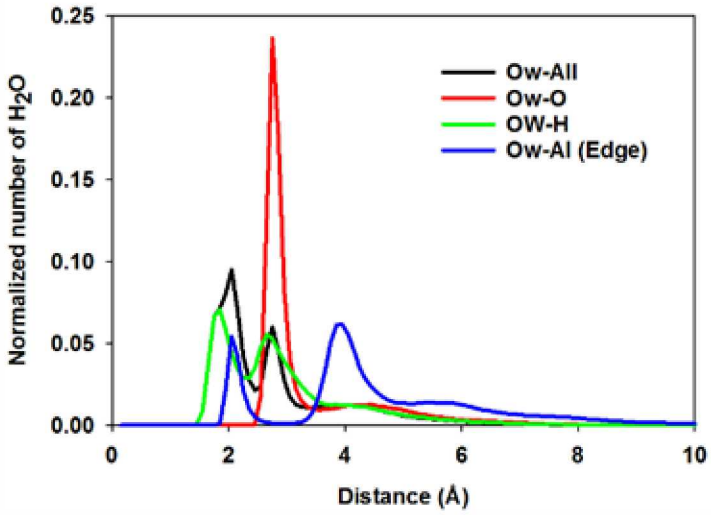

Distinct peaks due to water at basal vs edge surfaces.

Water structure at nanoparticle surfaces qualitatively the same regardless of water content.

- < 5 Å from surface: similar water coordination environments.
- > 5 Å from surface: pore water seen up to 10 Å from surface.

Ho, T.A. et al. (2017) Scientific Reports 7:15286

Summary of Gibbsite Nanoparticle Studies

- The percent cation adsorption as inner-sphere complexes depends on the gibbsite surface.
- For all cations, surface coverages are higher on the basal surface than the edge surface.
- For all cations, surface coverages are highest for the nanoparticle, due to the significant number of inner-sphere cations found at nanoparticle corners.
- For the nanoparticle aggregates, slow dewatering creates more compact aggregates that fast dewatering.
- For the aggregates, the amount of water present strongly affects the particle-particle interactions and the aggregate structure.

Objectives of Fracture Simulations

- Develop a fundamental, atomistic-level understanding of the *chemical-mechanical* processes that **control subcritical cracks** in low-permeability geomaterials.
- Link atomic-scale insight to macroscale observables.
- Address how **chemical environment** affects **mechanical behavior**.

- Rimsza, J.M., Jones, R.E. and Criscenti, L.J. (2019) Mechanisms of Silica Fracture in Aqueous Electrolyte Solutions. Frontiers in Materials 6.
- Rimsza, J.M., Jones, R.E. and Criscenti, L.J. (2018) Chemical Effects on Subcritical Fracture in Silica From Molecular Dynamics Simulations. Journal of Geophysical Research-Solid Earth 123, 9341-9354.
- Rimsza, J.M., Jones, R.E. and Criscenti, L.J. (2018) Crack propagation in silica from reactive classical molecular dynamics simulations. Journal of the American Ceramic Society 101, 1488-1499.

Geochemical Reactions in Subcritical Fracture

Subcritical fracture is an example of a nano-confined space – a location where the chemistry of reactions will be impacted by:

- Proximity of two surfaces
- Changes in water structure
- Changes in ion adsorption mechanisms

Fracture geometries are wedge-shaped, introducing the effects of nanoconfinement on geochemical fluids over a range of pore sizes from the tip to the bulk solution.

The chemical reactions that occur in a subcritical fracture impact the mechanical properties of the material and influence fracture propagation.

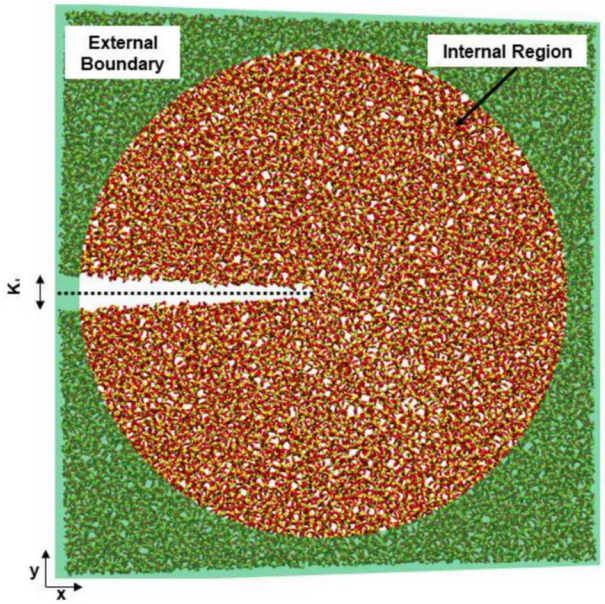

- Schematic of the quasi-2D silica system with a slit crack.
- Bonds are severed to form a slit crack.
- Atoms in the boundary region are fixed to the displacement proscribed by mode I loading
- Radius of cylinder = 3.2 nm
- In the cylindrical region, the atoms are free to relax to a minimum energy configuration
- The axis of the cylinder is out-of-plane and the thickness of the system is 2.8 nm.

Computational Methods

- Classical molecular dynamics for large scale simulation of silica fracture
- ReaxFF: Bond-order based forcefield including reactive water and silica bond breakage and formation (Fogarty et al. *J. Chem. Phys.* (2010), Yeon and van Duin, *J. Phys. Chem. C.* (2015)

$$E_{Total} = E_{Bond} + E_{Over} + E_{Under} + E_{LP} + E_{Val} + E_{Pen} + E_{Tors} + E_{Conj} + E_{VDW} + E_{Coul}$$

- 2D silica structures (12-replicates) were used.
- Investigated 3 different conditions to isolate chemical and mechanical effects on fracture
- Protocol: Apply initial loading (0.15 MPa$\sqrt{m}$) and relax fracture tip
  - Mechanical: increase loading (stepwise), relax for 5ps at 300K, repeat
  - Chemical-Mechanical: increase loading, add in water, relax for 5ps at 300K, repeat
  - Chemical: maintain loading, relax for 5ps at 300K, repeat

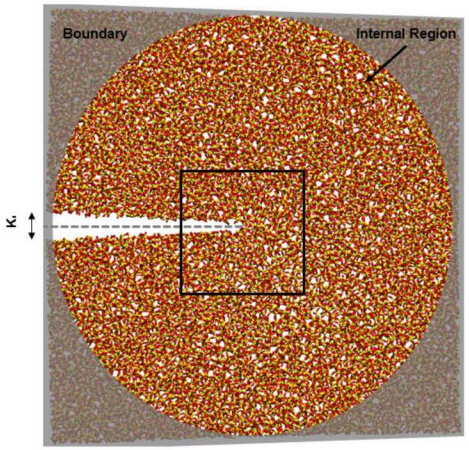

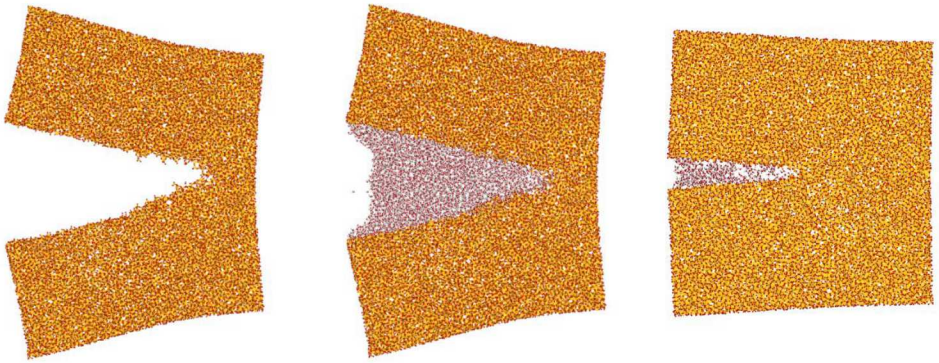

Mechanical
(mechanical loading only)

Chemical-Mechanical
(aqueous enviorment and mechanical loading)

Chemical
(aqueous enviorment only)

Fracture Toughness in Vacuum and Water

- Identified from variation in the potential energy of the silica during loading
- Earlier fracture of silica in aqueous conditions
- No fracture in chemical-only systems (dissolution)
- K_{IC} is lower than in experimental systems (0.78 MPa√m) due to resolution and temperature effects

Mechanical: 0.339±0.037 MPa√m
Chemical-Mechanical: 0.246±0.074 MPa√M
Reduction in K_{IC}: ~26.5%

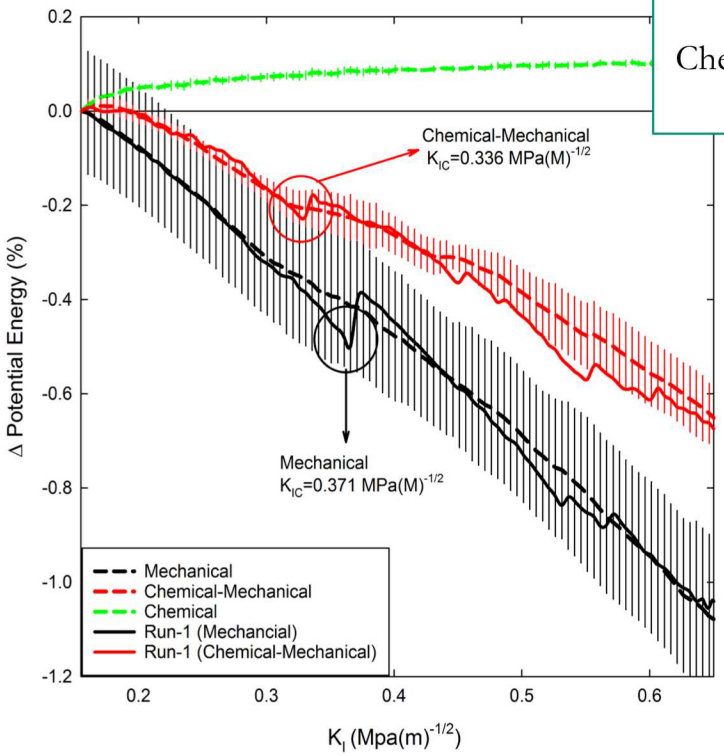

Change in potential energy for silica systems in mechanical, chemical, and chemical-mechanical conditions.

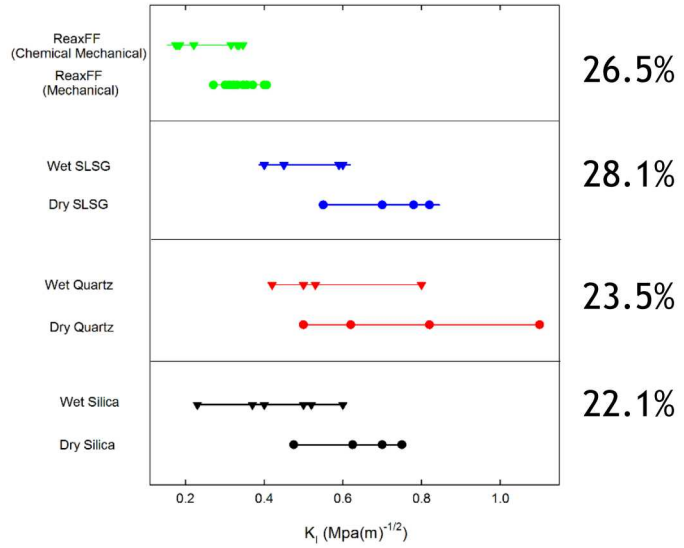

Experimental K_{IC} data for amorphous silica, quartz, and soda-lime silicate glasses in dry and aqueous environments compared with current data.

Fracture Propagation in Water

- Fracture depth identifies aggregate effect of aqueous environment on fracture
- Chemical-mechanical conditions: longer fracture propagation, larger number of fracture events and slightly shorter average fracture length
- Chemical effects become more prominent as the fracture propagates
- May be altering the conditions for fracture (bond stretching, stress states etc.)
- Chemical impact is more than additive on fracture growth

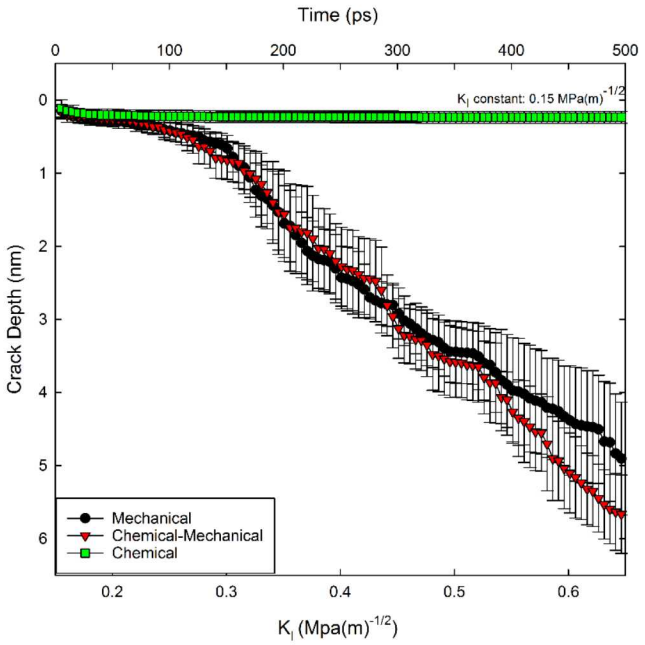

Crack depth for silica systems in mechanical, chemical, and chemical-mechanical conditions.

Crack propagation data for silica systems under different conditions.

Conditions	Propagation (nm)	Fracture Events* (#)	Average Fracture Length (nm)	Longest Fracture (nm)	Fracture Velocity (m/s)
Mechanical	4.92±0.76	11.50±2.06	0.35±0.08	0.90±0.23	9.85±1.51
Chemical	0.23±0.07	0.50±0.50	0.16±0.08	0.10±0.08	0.47±0.16
Chemical-Mechanical	5.69±0.53	14.83±2.41	0.32±0.06	0.97±0.38	11.38±1.07

Solution Composition in Fracture

OH^- Concentration in Solution

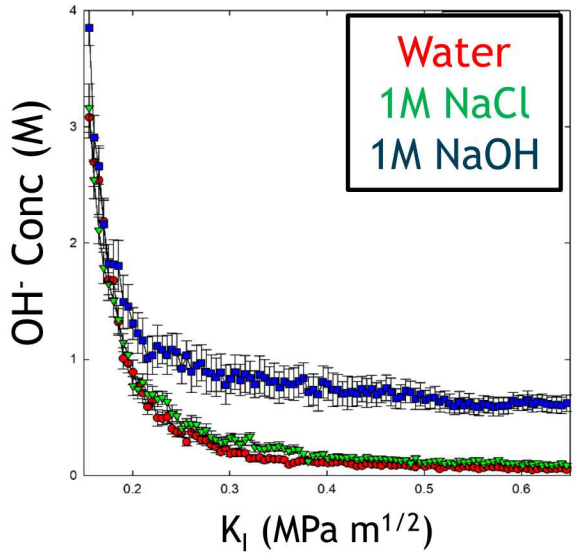

H_3O^+ Concentration in Solution

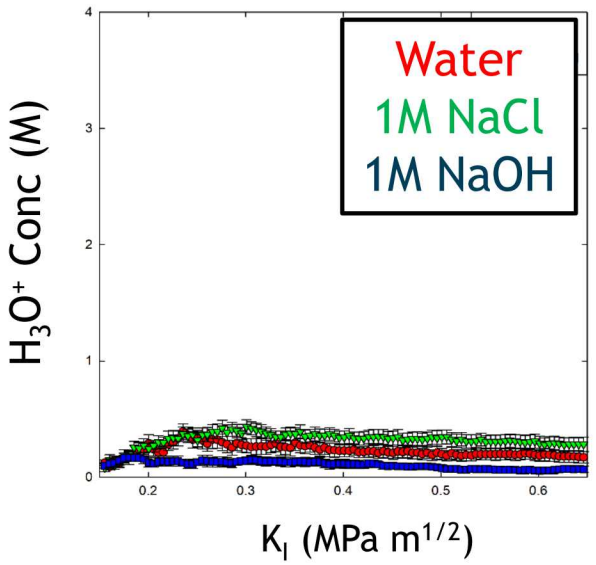

- Rapid change in concentrations occurs with initial loading before crack propagation
- Steady-state concentration occurs at ~0.25-0.3 MPa$\sqrt{m}$ due to balance of rate of water infiltration and addition of NaCl or NaOH molecules as fracture is loaded
- Concentration of H_3O^+ increases with decreasing pH: 1 M NaOH < water < 1 M NaCl.
- Silica dissolution should be higher in both NaCl and NaOH solutions than in pure water.

Accessibility of Fracture Tip to Different Ions

Water

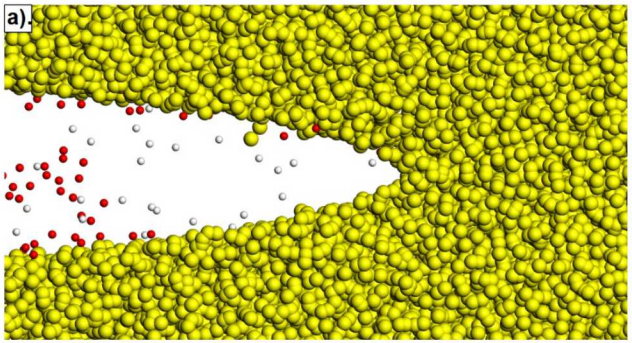

1M NaCl

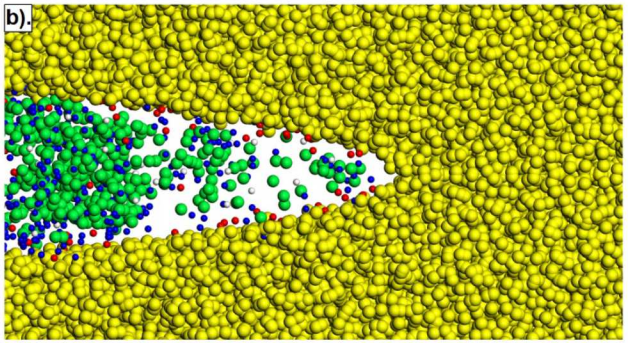

1M NaOH

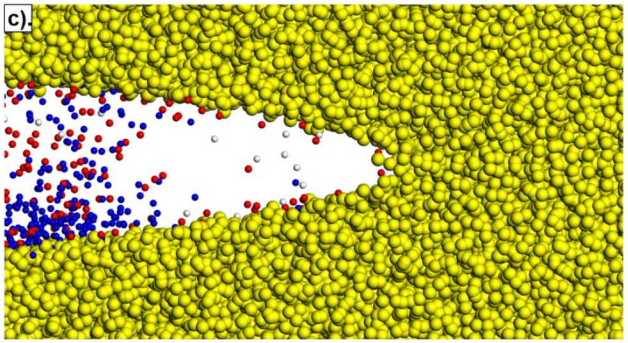

Si H_3O^+ OH^- Na^+ Cl^-

- NaCl and NaOH molecules were added at the widest point in the fracture to emulate diffusion of ions from the bulk fluid
- For silica fracture in H_2O, the crack tip is filled with H_2O and a few H_3O^+
- OH^- migrates to fracture tip in both NaCl and NaOH solutions
- In NaCl solutions, the tip is filled with Na^+, Cl^- and some OH^-, H_3O^+
- Limited Na^+ diffusion into crack tip from NaOH solution; crack tip contains surface coordinated OH^- or free H_3O^+.

Na^+ Coordination Structures

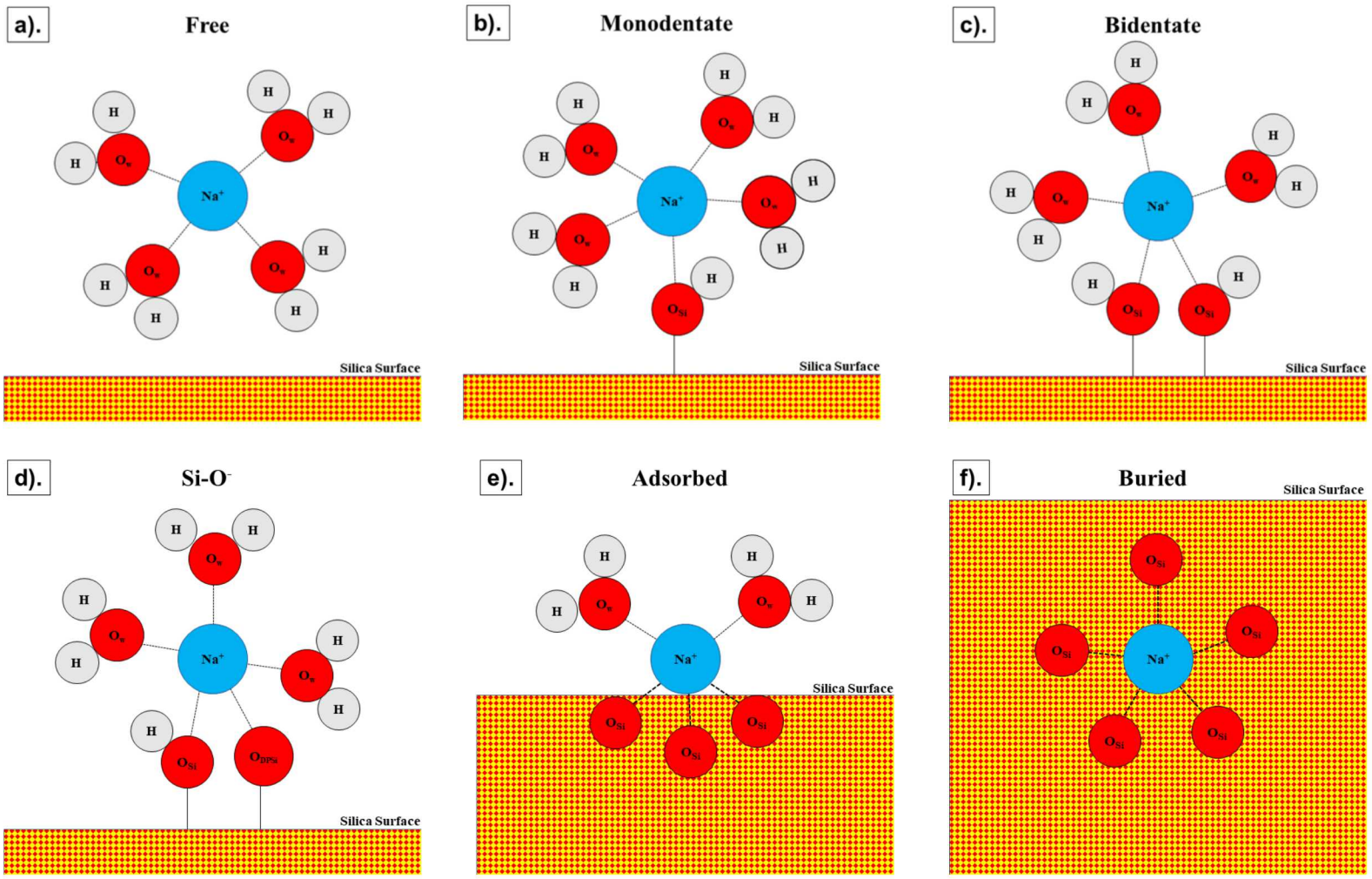

Structure (d) does not occur on flat surfaces: nanoconfinement effect of fracture tip

Fracture Properties of Silica for Different Environmental Conditions

	eK_{IC} (MPa$\sqrt{m}$)		Fracture Events (#)	G_{IC} (J/m^2)	G_{diss} (J/m^2)	Si-OH (#/nm^2)	γ (J/m^2)
	First	Average					
Vacuum	0.34±0.04	0.43±0.04	3.67±1.18	7.91	6.78	0.00	1.13
Water	0.20±0.06	0.37±0.05	4.33±1.03	4.59	4.21	3.10	0.38
1M NaCl	0.28±0.09	0.41±0.05	5.42±1.66	5.14	4.75	3.04	0.39
1M NaOH	0.19±0.05	0.37±0.05	6.00±1.41	5.47	5.06	2.95	0.41

Ranking of factors that influence environmentally assisted fracture

	eK^*_{IC}	Fracture events	Dissolution	Si-O$^-$ #	Tip access	Radius of curvature
Water	2	3	3	3	3	3
1M NaCl	1	2	1	2	1	1
1M NaOH	3	1	2	1	2	2

Summary of Silica Fracture

- Amorphous silica is substantially weaker when in contact with aqueous solutions than in vacuum due to chemical reactions with preexisting cracks.
- Fracture toughness is lowest for silica in 1M NaOH solutions. The basic solution leads to higher surface deprotonation, less dissolution, and a narrower radius of curvature than in an acidic environment.
- The 1M NaCl solution causes more silica dissolution than pure water or a 1M NaOH solution and changes the geometry of the fracture tip. In addition Q^0 silica species are observed in solution.
- The nanoconfinement at the fracture tip results in different Na^+ adsorption mechanisms than on a flat surface.

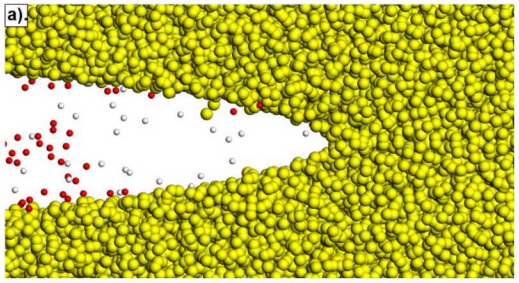

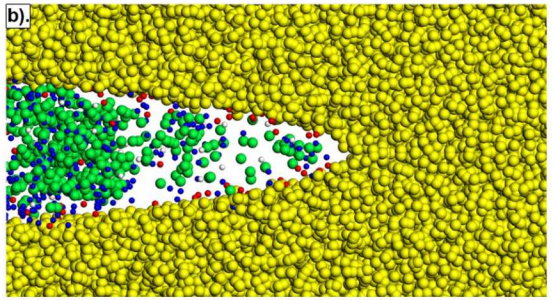

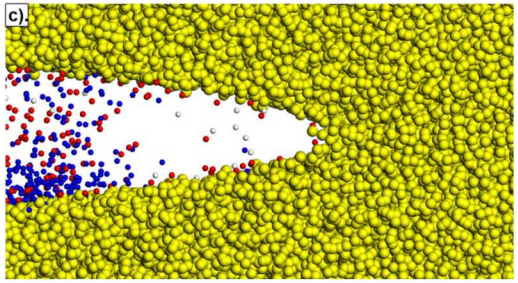

This work was fully supported by the Laboratory Directed Research and Development (LDRD) program of Sandia National Laboratories.

Future Work: Chemo-Mechanical Fracture in Aggregates (i.e., Rocks)

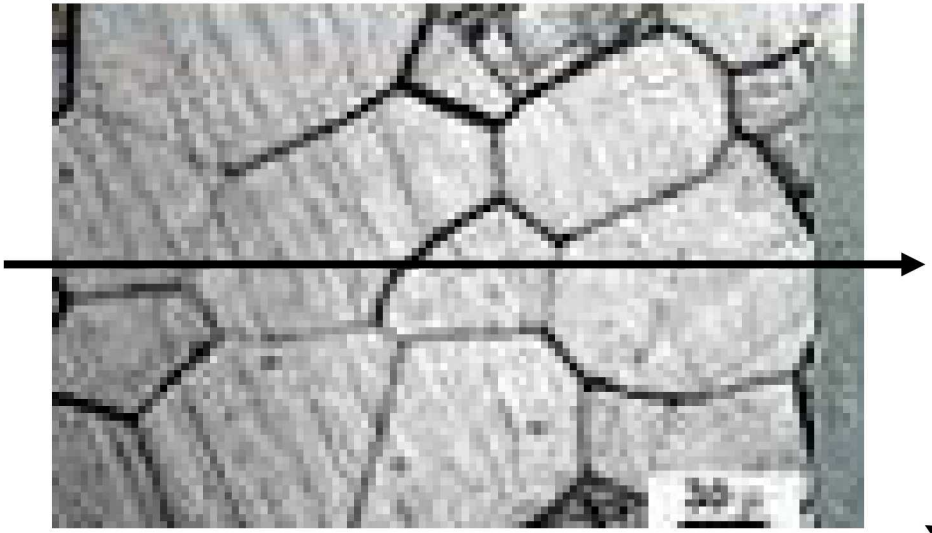

When will fracture go through grains rather than around grains? Will solution composition have an impact on this?

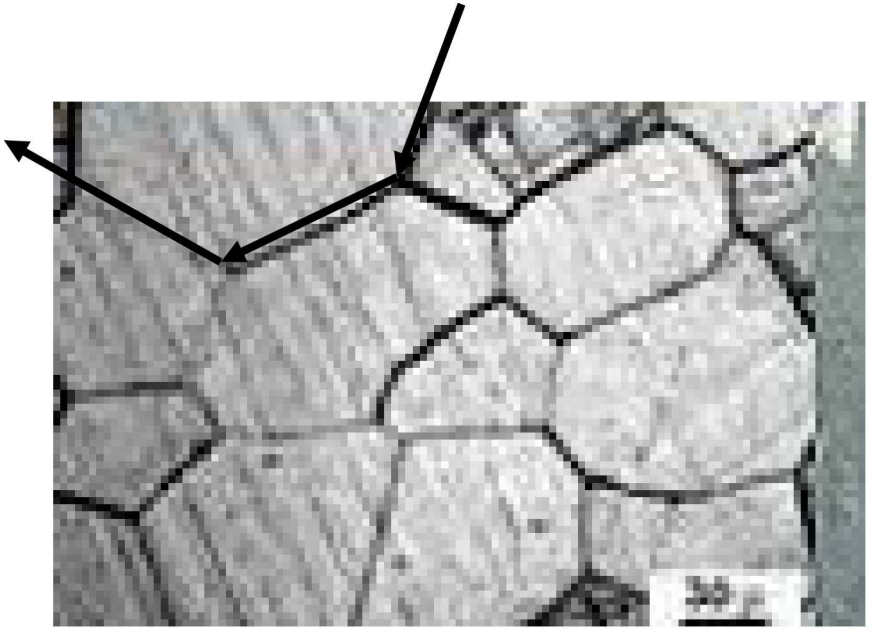

EXTRA SLIDES